HHS Public Access

Author manuscript

Oncogene. Author manuscript; available in PMC 2011 July 20.

Published in final edited form as:

Oncogene. 2011 January 20; 30(3): 301–312. doi:10.1038/onc.2010.412.

Control of mammary tumor differentiation by SKI-606 (bosutinib)

Lionel Hebbard, Ph.D.[1,7], **Grace Cecena, B.S.**[1], **Jonathon Golas, Ph.D.**[2], **Junko Sawada, Ph.D.**[4], **Lesley G. Ellies, Ph.D.**[5], **Adriana Charbono**[1], **Roy Williams, Ph.D.**[1], **Rebecca E. Jimenez**[6], **Miriam Wankell, Ph.D.**[1], **Kim T. Arndt, Ph.D.**[2], **Susan Q. DeJoy, Ph.D.**[2], **Robert A. Rollins, Ph.D.**[2], **Veronica Diesl, Ph.D.**[2], **Maxmillian Follettie, Ph.D.**[2], **Lei Chen, Ph.D.**[2], **Edward Rosfjord, Ph.D.**[2], **Robert D. Cardiff, M.D, Ph.D.**[3], **Masanobu Komatsu, Ph.D.**[4], **Frank Boschelli, Ph.D.**[2], and **Robert G. Oshima, Ph.D.**[1,*]

[1]Cancer Research Center, Sanford-Burnham Medical Research Institute, La Jolla, CA 92037

[2]Center for Integrative Biology and Biotherapeutics, Pfizer Research, Pearl River, New York 10956

[3]Center for Genomic Pathology University of California, Davis, CA

[4]Sanford-Burnham Medical Research Institute, Lake Nona, Fla

[5]Pathology Department, University of California, San Diego

[6]Biomedical Science Program, University of California, San Diego La Jolla, CA

Abstract

C-Src is infrequently mutated in human cancers but it mediates oncogenic signals of many activated growth factor receptors and thus remains a key target for cancer therapy. However, the broad function of Src in many cell types and processes requires evaluation of Src-targeted therapeutics within a normal developmental and immune-competent environment. In an effort to understand the appropriate clinical use of Src inhibitors, we tested a Src inhibitor, SKI-606 (bosutinib), in the MMTV-PyVmT transgenic mouse model of breast cancer. Tumor formation in this model is dependent on the presence of Src, but the necessity of Src kinase activity for tumor formation has not been determined. Furthermore, Src inhibitors have not been examined in an autochthonous tumor model that permits assessment of effects on different stages of tumor progression. Here we show that oral administration of SKI-606 inhibited the phosphorylation of Src in mammary tumors, and caused a rapid decrease in the Ezh2 Polycomb group histone H3K27 methyltransferase and an increase in epithelial organization. SKI-606 prevented the appearance of palpable tumors in over 50% of the animals and stopped tumor growth in older animals with preexisting tumors. These antitumor effects were accompanied by decreased cellular proliferation,

[*]Corresponding author: Sanford-Burnham Medical Research Institute 10901 N. Torrey Pines Road, La Jolla, CA 92037 rgoshima@burnham.org Phone: 858-646-3147.

[1,4]formerly Burnham Institute for Medical Research

[2]formerly Wyeth Oncology Discovery Research

[7]current address: Westmead Millennium Institute, Storr Liver Unit, Westmead NSW 2145, Australia

Conflict of Interest - The following authors: Kim Arndt, Frank Boschelli, Lei Chen, Susan Q. DeJoy, Veronica Diesl, Maxmillian Follettie, Jonathan Golas, Robert Rollins and Edward Rosfjord are employees of Pfizer (formerly Wyeth Research), which is pursuing clinical development of bosutinib. All the remaining authors declare no conflicts of interest.

altered tumor blood vessel organization and dramatically increased differentiation to lactational and epidermal cell fates. SKI-606 controls the development of mammary tumors by inducing differentiation.

Keywords

Src; SKI-606; mouse; breast cancer; Ezh2

Introduction

In breast cancer, Src is of particular interest because it is activated by both steroid hormone receptors and ErbB family growth factor receptors, and activates transcription factors such as STAT3, STAT5 and β-catenin by direct phosphorylation (Kim *et al.*, 2009; Silva and Shupnik, 2007). Cellular Src was discovered in 1978 as the cellular counterpart of a viral gene, *v-src*, the transforming agent of Rous sarcoma virus (Spector *et al.*, 1978). This non-receptor tyrosine kinase belongs to a family of proteins that mediate signaling by a large number of growth factor receptors, integrins, G-protein coupled receptors, hormones and stress responses implicated in multiple types of cancer and vascular biology (Criscuoli *et al.*, 2005; Kim *et al.*, 2009; Summy and Gallick, 2006). Src is over-expressed and activated in many human cancers, including breast cancer, and activation generally correlates with poor prognosis. Nonetheless, biomarkers predictive of a clinical response remain elusive.

The Src inhibitors dasatinib, saracatinib (AZD0530), and SKI-606 (bosutinib) are in Phase II clinical development for the treatment of solid tumors of metastatic breast and prostate cancer. SKI-606, a multikinase inhibitor originally identified as a Src and Abl kinase inhibitor, is effective in vitro on colorectal and breast tumor cells, chronic myelogenous leukemia cells and also in multiple xenotransplantation experiments (Boschelli *et al.*, 2001; Jallal *et al.*, 2007; Vultur *et al.*, 2008). Src inhibitors generally have subtle effects on tumor cells under normal culture conditions (Golas *et al.*, 2005; Vultur *et al.*, 2008). The effects of SKI-606 in models of developing breast cancer has not been reported

The many functions of Src and Src family kinases in multiple signaling pathways suggests that the effects of inhibiting Src should be integrated into a whole animal context with a fully functional immune system (Finn, 2008). The Src-dependent, immunocompetent, autochthonous FVB/N-Tg(MMTV-PyVmT)634Mul (MMTV-PyMT) breast cancer mouse model is an ideal tool for such a study because it permits the evaluation of both early and late stages of luminal type metastatic carcinomas (Guy *et al.*, 1992; Lin *et al.*, 2003). This model mimics changes associated human breast cancer progression including up regulation of cyclinD1 and HER2, and infiltration of leukocytes. PyMT-induced mammary tumors are dependent on multiple signaling molecules, including c-Src, phosphatidylinositol-3-kinase, Shc and Insulin/IGF-1 receptors (Ishizawar and Parsons, 2004).

Genetic inactivation of the c-*src* gene in MMTV-PyMT mice limits the effect of PyMT transgene expression to formation of hyperplastic lesions in mammary tissues after a long latency period with activated levels of c-Yes, a closely related member of the Src family of kinases (Guy *et al.*, 1994). C-Src activation by PyMT is not the sole driver for

tumorigenesis, since expressing activated Src under the MMTV-promoter in the absence of PyMT leads to defective mammary development and hyperplasia, but not invasive tumor formation (Webster *et al.*, 1995). Similarly, when PyMT is mutated to block either SHC or PI3-kinase association, only hyperplastic lesions are formed, (Webster *et al.*, 1998) unless an angiogenic stimulus such as VEGF is provided (Oshima *et al.*, 2004).

Our studies show that SKI-606 treatment suppressed both early hyperplastic stages of the disease and overt tumor development. SKI-606 treatment stopped growth of established tumors by inducing dysplastic differentiation of tumor cells and altered vascular organization. These responses were accompanied by downregulation of the Polycomb repressor complex 2 subunit EZH2. The control of this aggressive model of breast cancer by differentiation suggests that different clinical end points might be considered to evaluate drugs that control cancer via differentiation rather than cell death.

Results

SKI-606 inhibits cell growth in culture without inducing cell death

Previous studies indicated that treatment with 1 uM SKI-606 significantly reduced phosphorylation of the Y418 gatekeeper residue of c-Src in human tumor cells (Golas *et al.*, 2005; Vultur *et al.*, 2008). To determine whether SKI-606 affected in vitro growth of PyMT-transformed mammary tumor cells, Py-230 cells were treated with SKI-606 at various concentrations. In a 4-day assay, submicromolar concentrations of SKI-606 inhibited Py-230 cell proliferation (Fig. 1A). However Py-230 cells formed colonies from single cells in the presence of up to 750 nM SKI-606 (Fig. 1A), but colony size was significantly reduced (Fig. 1B), suggesting that SKI-606 inhibited proliferation of Py-230 cells without significant cytotoxic effects. Phosphorylation of Src^{Y418} was inhibited by 1 uM SKI-606 without affecting the total amount of Src protein (Fig. 1A, right, lane 3) while 0.1 uM SKI-606 had little effect. Y418 phosphorylation is required for full activity (Kmiecik and Shalloway, 1987) and thus, the extent of Y418 phosphorylation is an estimate of the maximum required concentration of a compound that fully inhibits Src.

SKI-606 accumulates in tumor tissue and inhibits Src activity

Previous published data indicated that orally administered SKI-606 was well distributed in the tissues of nude mice and accumulated in human tumor xenografts. Analysis of plasma obtained from MMTV-PyMT tumor-bearing mice 18 hours after a single oral dose of SKI-606 revealed plasma concentrations of 321 ng/ml (604 nM), well above the concentration effectively inhibiting Src kinase activity (Boschelli *et al.*, 2001) and well within the range required to inhibit breast cancer tumor cell growth and invasion in cell culture (Jallal *et al.*, 2007; Vultur *et al.*, 2008) (Fig. 1C). In addition, SKI-606 accumulates in PyMT tumors to a concentration of 2477 ng/g of tumor (Fig. 1C). We determined the relative levels of active Src in these tumors by monitoring the phosphorylation of Y418 18 hours following SKI-606 administration. SKI-606 treatment reduced P-Y418 levels in PyMT tumors by 75% of the levels observed in tumors from vehicle-treated animals (Fig. 1D), suggesting that SKI-606 inhibits the intended molecular target.

SKI-606 suppresses mammary tumor appearance

PyMT expression occurs about four weeks after birth upon mammary gland development at sexual maturity. The mammary epithelial tree of MMTV-PyMT adolescent females develops a small tumor-like mass beneath the nipple area concurrent with the emergence of the normal epithelial branching tubes (Maglione *et al.*, 2001; Neznanov *et al.*, 1999). Next focal hyperplastic lesions arise among the normal epithelial structures, which then progress to mammary intraepithelial neoplasia (MIN) and later to invasive cancer (Lin *et al.*, 2003; Maglione *et al.*, 2001).

Two groups of female MMTV-PyMT mice were administered SKI-606 (150 mg/kg) or vehicle by oral gavage at age 30 ± 2 days for up to 45 additional days on a schedule of five consecutive daily treatments followed by two days without treatment. All animals tolerated SKI-606 administration and SKI-606-treated animals could not be distinguished from the control group by weight (Fig. 2). All control animals developed palpable tumors at ages between 38 and 55 days (Fig. 2B). No tumors were detected in SKI-606-treated mice until an age of 60 days and only half of the treated animals developed obvious tumors by 75 days. Upon termination of treatment, only a few SKI-606 treated mice had tumors that could be recovered by dissection and none of these animals developed metastases in the lungs. The entire mammary glands of animals without grossly apparent malignancies were dissected from both groups and compared by weight. Figure 2C shows that SKI-606 treatment resulted in less dense mammary tissue than that observed with tissue from vehicle treated animals (P=0.002). Histological analysis revealed that mammary glands from SKI-606-treated animals had large fluid-filled cysts (Fig. 2D-d, 2D-e), containing abundant casein protein (Fig. 2D-f). Control tissue contained solid masses of typical MMTV-PyMT tumor cells (Fig. 2D-a, 2D-b). Reduced levels of casein were found in the vehicle control tumors (Fig. 2D-c) with a less extensive distribution. These results revealed SKI-606's remarkable anti-tumor efficacy with less than half of the animals developing overt, discrete tumors in this highly aggressive tumor model. Furthermore, mammary glands from SKI-606-treated mice had dysplastic but more differentiated cystic structures containing milk protein.

Tumors from SKI-606 treated mice are differentiated

To test the effect of SKI-606 treatment on developed mammary tumors, animals with tumor sizes of 0.6 to 1 cm in diameter were treated 14 consecutive days. Tumors of control animals continued to grow steadily with increasing variability in tumor size over time (Fig. 3A). In contrast, tumors in SKI-606-treated mice did not increase in size. After two weeks of treatment, the excised tumor weights were approximately half that of tumors from the control group (Fig. 3B). Staining of proliferative cell nuclear antigen (PCNA) revealed that tumors from SKI-606-treated mice were not as mitotically active (Fig. 3C). Histological examination showed the typical high nuclear density and undifferentiated state of PyMT tumors (Fig. 3-a, 3D-b, 3D-g). By contrast, SKI-606-treated tumors were heterogeneous with areas of higher nuclear density mixed with more epithelial glandular and papillary type structures (Fig. 3D-c, 3D-d). Some tumors had cysts lined by stratified squamous epithelium that produced copious laminated keratin debris. This type of differentiation has been previously observed with some types of MMTV-PyMT crosses and in Wnt-induced mammary tumors (Miyoshi *et al.*, 2002; Rosner *et al.*, 2002). Cystic areas of the tumors also

contained abundant beta-casein protein (Figure 3D-h). Of six animals of each group inspected for lung metastases, five of each group were found to have metastases. The 2-week SKI-606 treatment did not change the average of three metastases per lung per group, which likely existed before treatment start (Kouros-Mehr *et al.*, 2008). The sizes of the metastases were similar in both groups. The small size of most of the metastases prevented a definitive conclusion concerning differences in differentiation state.

PyMT tumors develop as expansions of keratin 8 (K8)-positive luminal epithelial cells lined by some keratin 14 (K14)-positive myoepithelial cells at early stages (Fig. 4A). The cystic structures induced by SKI-606 treatment contained both luminal K8-positive epithelial cells and K14-positive basal-like cells. These structures of SKI-606-treated tumors differed from normal mammary glands by occasional penetration of the luminal layer with K14-positive cells (Supplemental data, Fig. S2A) and by the lack of smooth muscle actin staining in the K14 cell layer (Supplemental data, Fig. S2C). This differentiated state was not accompanied by an increase in apoptosis assessed by DNA end labeling (Fig. S2B). Furthermore, ER was found associated with the highly proliferative outer rim of tumors and within stromal cells (Fig. S2D). The nuclear ER at the outer margin of tumor masses and within many of the organized epithelia was not diminished by SKI-606 treatment (Fig. S2D).

SKI-606 treatment induces remodeling of mammary tumor vasculature

To determine the impact of SKI-606 on PyMT tumor vascularity, we stained tumor sections with anti-CD31. The vascular network of the vehicle-treated tumors displayed a chaotic organization (Fig. 4C, left). Control tumor vessels were largely dilated and the endothelium was thick or extended resulting in severe vessel deformation. These vessel abnormalities are hallmarks of the tumor vasculature (Cheung *et al.*, 1997; Jain, 2005). SKI-606 treatment resulted in significant remodeling of the tumor vasculature after 14 days of treatment. The vascular network of SKI-606-treated mammary tumors exhibited reduced dilation (Fig. 4C, D) and a thinner vessel endothelium (Fig. 4C, right), minimizing vessel deformation. Furthermore, the vessels in the SKI-606-treated tumors appeared to be more evenly distributed than those in control tumors (Fig. 4C). While SKI-606 induced significant structural remodeling of the vessels, it did not affect the overall tumor vessel density (Fig. 4D, right). SKI-606 treatment may directly or indirectly induce normalization of the tumor vasculature as observed in the vascular normalization phenomenon induced by VEGF blockade-based antiangiogenic therapies (Jain, 2005).

Gene expression changes associated with SKI-606 treatment

The RNAs of eight tumors each from SKI-606- and vehicle-treated mice each were analyzed for gene expression changes on two different array platforms (Illumina bead arrays, Affymetrix arrays) to identify the most robust gene expression changes. Data are available from the GEO accession numbers GSE20921 and GSE22150. Given the histological variation, the list of genes that were significantly changed in both arrays was small (Table S1). Comparison of the 34 genes altered by SKI-606 treatment to other array results resulted in identifying multiple studies with similar gene expression changes (Table S2). In four examples, SKI-606-induced genes were decreased in cancer cells. Increased expression of these genes in SKI-606 treated tumors is consistent with reversing the cancer phenotype.

Twelve of the 34 SKI-606-induced genes were increased in lactating normal mammary gland. These results are consistent with the increased casein level and increased epithelial differentiation of SKI-606-treated tumors. Examination of keratin gene expression in individual tumors and their corresponding histological appearance revealed that increased expression of keratin genes was associated with only three of the eight tumors (Fig. 5A and B). However, each of those tumors with increased K5, K7, K14 and K17 also had areas of epidermal-like differentiation (Fig. 5C, tumors 737, 787 and 698). These results suggest that PyMT tumors do not respond uniformly to SKI-606 but rather may adopt distinct differentiated fates or respond asynchronously depending on their particular microenvironment.

Western blot analysis of four of six serum samples from tumor-bearing animals treated with SKI-606 for 14 days had elevated casein protein levels while none of the six samples from tumor-bearing control mice showed similar casein levels (Supplemental data, Fig. S5). The casein signal was comparable to serum levels found in lactating mothers (Supplementary data, Fig. S5B, lanes 8, 9). These results suggest a blood test may provide information about the differentiation response.

SKI-606 treatment reduces Ezh2 expression

The Ezh2 polycomb group protein expression is elevated in aggressive human breast cancers (Kleer *et al.*, 2003) and increased expression is associated with reduced E-cadherin levels (Cao *et al.*, 2008). SKI-606 treatment increases E-cadherin stability in colorectal tumor cells and E-cadherin localization at the plasma membrane in several cell types (Jallal *et al.*, 2007; Vultur *et al.*, 2008) (Coluccia *et al.*, 2006). Given these relationships, and the profound responses in the SKI-606-treated mice, we examined the effects of SKI-606 on Ezh2 levels.

Ezh2 levels of tumors 18 hours after a single dose of SKI-606 were measured by immunoblot analysis. Ezh2 levels were reduced by approximately 50% in SKI-606-treated samples (Fig. 6A, 6B). In addition, RT-PCR analysis of RNA from tumors excised from mice 8 hours after SKI-606 administration revealed a 50% reduction of Ezh2 mRNA (Fig. 6B). E-cadherin mRNA levels increased after a single treatment with SKI-606 (Fig. 6B). Immunohistochemical analysis revealed high and nearly uniform expression of Ezh2 in the MMTV-PyMT tumor lobes. This expression was decreased in tumors from animals treated with SKI-606 just once (Fig. 6C-a), (Supplementary data, Fig. S4). Furthermore, decreased Ezh2-staining appeared to correlate with portions of the tumors that had adopted a more epithelial morphology (Figure 6C-c, 6C-d, arrows). In tumors treated for 14 days, Ezh2 was greatly diminished (Fig. 4B; supplementary Fig. S3). E-cadherin staining was very strong in the differentiated epithelial cysts formed following 14 days of treatment (Fig. 4B) (Supplementary Fig. S3). In tumor samples with epidermal differentiation, Ezh2 was localized in the presumptive proliferative cells surrounding the focal keratin differentiation. E-cadherin localization appeared adjacent to Ezh2 in these areas (Supplementary data, Fig. S3, sample 2241). This organization of Ezh2 and E-cadherin is similar to that observed during normal epidermal development (Ezhkova *et al.*, 2009). These data show that a key developmental regulatory protein decreases rapidly after SKI-606 exposure and its loss is associated with increased E-cadherin RNA and more organized epithelium.

Discussion

Treatment of adolescent MMTV-PyMT females for four weeks effectively prevented palpable tumor formation in half of the SKI-606 treated animals. Instead of residual solid tumors, distended, dysplastic mammary cysts with accumulated casein protein filled the fat pads. The differentiation-inducing effect of SKI-606 was most dramatically demonstrated by the 2-week treatment of tumor-bearing animals. This resulted in enrichment of organized K14-positive basal epithelia juxtaposed with luminal epithelial cells in cystic structures, the accumulation of milk protein and sporadic epidermal differentiation. Strikingly similar observations of cystic buildup of milk proteins were reported for Src null mice, which were ascribed to a defect in secretory activation during pregnancy (Watkin *et al.*, 2008).

The relatively small list of differentially expressed genes in SKI-606 treated tumors is likely because of the variation of the differentiation of individual tumors that decreased the probability of passing multiple statistical thresholds. Genes whose expression was increased in all SKI-606-treated tumors overlap significantly with genes increased during lactation (Rudolph *et al.*, 2007) and repressed in mouse transgenic tumors caused by c-Myc, SV40 T antigen and ETV6-NTRK3 (Bild *et al.*, 2006; Klein *et al.*, 2005; Li *et al.*, 2007) and human breast cancer cell lines (Klein *et al.*, 2005). These results suggest that the SKI-606 induced differentiation reflects the reversal of a common transcriptional response to oncogene transformation. The induction of differentiation by SKI-606 may be related to the function of Src in ER signaling (Ishizawar and Parsons, 2004). Cross talk between ER and Src is well documented and may include effects on the nuclear localization of ER. Src null mice have defects in mammary gland development and ER signaling (Kim *et al.*, 2005b). While we found no differences in the cellular distribution of ER in both tumor cells or in stromal cells of mice treated with SKI-606, alterations in ER activity may still contribute to the diverse differentiation responses observed.

Differentiation of SKI-606-treated PyMT tumors was associated with changes in vascular organization, although not vascular density. Src is involved in the production of VEGF (Mukhopadhyay *et al.*, 1995) and Src is activated by VEGF receptors (Eliceiri *et al.*, 1999). Significantly, the observed changes in vascular organization after SKI-606 treatment are consistent with normalization of the more permeable and tortuous vessels found in these tumors (Cheung *et al.*, 1997). SKI-606 treatment reduces tumor cell extravasation (Weis *et al.*, 2004) at least in part by strengthening VE-cadherin (cadherin 5) and beta-catenin interaction. SKI-606 was also effective in models for ischemic stroke where VEGF-induced vascular leakage mediated by Src activation is believed to play a dominant role in disease etiology. These observations suggest that Src inhibition by SKI-606 contributes to tumor vascular normalization. While SKI-606 was originally developed as a Src inhibitor, subsequent studies indicated that it targets multiple kinases including Abl kinases (Remsing Rix *et al.*, 2009). At the RNA level, Lck, Egfr and Csk are expressed at detectable levels in PyMT tumors and are reported to have SKI-606 IC_{50} of 100 nM or less (Remsing Rix et al. 2009). However, the observed biological responses to SKI-606 treatment are consistent with existing knowledge of the roles of Src in angiogenesis, tumor cell survival, proliferation and motility (Finn, 2008). Src inhibition alone may be responsible for a large part of the observed biological effect on these tumors.

Apoptosis outside of obviously necrotic areas was not increased significantly in tumors treated for either 18 hours (data not shown) or two weeks. Thus, the response of tumor cells to SKI-606 appears to be decreased proliferation but not elevated cell death. Within tumor cells, Src binds to and mediates the oncogenic signaling of Polyoma middle T antigen (Courtneidge and Smith, 1983). While the presence of Src is required for PyMT-induced tumors to form in the mammary gland (Guy *et al.*, 1994), deleting Src is not equivalent to inhibiting its kinase activity, as demonstrated by partial restoration of osteoclast function by expression of catalytically inactive Src in Src-deficient osteoclasts (Schwartzberg *et al.*, 1997). SKI-606 treatment for 4 weeks resembles the result of genetically inactivating Src. This is consistent with Src inhibition being an important mediator of the effects of SKI-606.

PyMT activates both Src and PI3 kinase pathways, much like the combination of ErbB2 and ErbB3 signaling. Src is also activated by ErbB2 receptor signaling (Muthuswamy *et al.*, 1994), directly associates with the same receptor (Kim *et al.*, 2005a) and facilitates the heterodimerization of ErbB2 and ErbB3 (Ishizawar *et al.*, 2007). Thus, SKI-606 might be expected to have similar effects on ErbB2-driven mammary tumors as those observed here for PyMT-driven tumors.

Ezh2 is a core component of the Polycomb Repressive Complex 2 (PRC2), that mediates gene repression by methylating lysine 27 on histone H3 and recruiting histone deacetylase (Bracken and Helin, 2009). PRC2 may maintain pluripotency by silencing developmental regulators that drive differentiation (Lee *et al.*, 2006). Poorly differentiated human tumors show preferential repression of PRC2-regulated genes and this expression pattern is associated with poor clinical outcome. There is a strong correlation between elevated Ezh2 levels and poorly differentiated breast carcinomas (Kleer *et al.*, 2003). Deregulated expression of Ezh2 and its downstream target genes may play a critical role in maintaining the arrested differentiation phenotype observed in aggressive tumors.

Treatment of MMTV-PyMT tumors with SKI-606 resulted in a rapid reduction in Ezh2 protein, and a modest increase in E-cadherin mRNA, as might be expected from the transcriptional inhibition of the E-cadherin promoter by Ezh2, (Cao *et al.*, 2008). However, E-cadherin protein and RNA are expressed within PyMT tumor cells suggesting that EZH2 is not sufficient to silence E-cadherin in this system. SKI-606 may alter Ezh2 levels indirectly through miR-101; a group of microRNAs that have been shown to negatively regulate Ezh2 levels (Varambally *et al.*, 2008). The relatively rapid inhibition of Ezh2 expression following SKI-606 treatment is consistent with a functional and early role of Ezh2 rather than only a reflection of the later differentiated state of treated tumors. This is not likely due only to an anti-proliferative effect because a single treatment with SKI-606 for 18 hours did not result in a significant decrease in PCNA labeling index (not shown), even though Ezh2 protein was clearly decreased. Over-expression of Ezh2 in the mouse mammary epithelium leads to intraductal hyperplasia and delayed involution (Li *et al.*, 2009). Similarly, MMTV-driven expression of activated Src causes mammary hyperplasia and arrested lobuloalveolar development (Webster *et al.*, 1995), suggesting that both proteins may cooperate to restrict the cell fates and maintain the undifferentiated cellular phenotypes that are common in aggressive breast cancers. The restriction of MMTV-PyMT tumors by SKI-606 induced differentiation may be mediated by both tumor and host cell

responses. The restriction of mammary tumor progression by induced differentiation is a relatively rare example that stimulates consideration of differentiation therapy. It will be of great interest to determine the link between Src inhibition and Ezh2 expression in developing breast cancer.

Materials and Methods

Antibodies

The antibodies used were: keratin 8 (TROMA1, Developmental Studies Hybridoma Bank, University of Iowa); keratin 14 (Covance, PRB-155P); CD31 (Pharmingen, 01951D, BD Bioscience), PCNA (Sigma, P8825), smooth muscle actin (Sigma, C6198), EZH2 (6A10, Novocastra and AC22, Cell Signaling). E-Cadherin, Clone 24E10, (Cell Signaling Technologies) and Alexa 488 donkey anti-rabbit IgG (Molecular Probes A21206), Alexa 568 goat anti rat IgG (Invitrogen 11077), HRP anti-mouse IgG (DAKO Envision system) and anti-rabbit IgG (Vector ImmPRESS).

The Py-230 cell line was isolated from a MMTV-PyMT tumor by Dr. Leslie Ellies and grown in F12K media (Mediatech), supplemented with 5% fetal bovine serum and MITO growth factor supplement (Fisher CB50006). Cell numbers were determined by imaging methanol-fixed cells grown for 4 days in 96-well plate stained with DAPI using the Beckman IC-100 imagining equipment and Cytoshop software. Data of nine images per well and triplicate wells were used to calculate total cell numbers.

Animal procedures

The transgenic MMTV-PyMT mouse on the FVB/N genetic background was obtained from Dr. William Muller (Guy *et al.*, 1992). Genotypes were determined previously described (Man *et al.*, 2003). Tumor analysis was performed as previously described (Liu *et al.*, 2005; Neznanov *et al.*, 1999). SKI-606 was formulated in 0.5% methocellulose and 0.4% Tween 80 and administered by oral gavage at 150 mg/kg. Hyperplastic areas of whole mounted mammary glands were measured from images converted to gray scale. Total pixel areas of threshold images were measured using Image J software. Statistical tests were performed within the Prism® suite of tests. SKI-606 levels in plasma were determined as previously described (Boschelli et al., 2001).

Histology

Apoptosis was detected using terminal deoxynucleotidyl transferase-mediated dUTP nick end-labeling of hydrolyzed nuclear DNA, (ApopTag, Millipore Co). Antigen retrieval was performed in citrate buffer, pH 6 on zinc-formalin (Z-fix, Anatech, Battle Creek MI) fixed paraffin embedded tissues. K8, K14, smooth muscle actin and CD31 were detected with acetone-fixed, sucrose infused, OCT embedded, frozen sections. Volocity software (Improvision) was used to determine blood vessel area, perimeter, and density. Four tumors were analyzed for each group using seven random areas from each tumor section. Over 3,000 tumor blood vessels were individually analyzed in total for each group.

Protein and RNA analysis

Immunoprecipitation and western blot analysis was performed as described (Jallal *et al.*, 2007). Quantitative real-time PCR was performed with FAM-labeled TaqMan probe sets specific for mEzh2 (Mm00468464_m1) or beta-Actin (Mm01205647_g1) from Applied Biosystems. Cdh1 RNA was independently measured using methods that were previously described (Galang *et al.*, 2004).

Gene Expression Array analysis

RNA was analyzed with Illumina MouseRef-8 BeadChips using the manufacturer's BeadArray Reader and Scanner and BeadStudio software. In addition, an additional set of tumors from control and test groups was analyzed using Affymetrix chips and procedures. Data analysis was done in three stages. First, expression intensities were calculated for each gene probed on the array for all hybridizations (26 in total) using Illumina's Beadstudio #1 software. Second, intensity values were quality controlled and normalized: quality control was carried out by using the Illumina Beadstudio detection P-value set to be 0.1 as a cutoff. This removed genes that were not detected. All the arrays were then normalized using the normalize quantiles routine from the Affymetrix package in Bioconductor. These normalized data were imported into GeneSpring and analyzed for differentially expressed genes. The groups of biological replicates were described to the software, and significantly differentially expressed genes were determined based on t-tests and fold difference changes in expression level. Primary data is deposited in GEO database under accession numbers: GSE20921 and GSE22150.

Supplementary Material

Refer to Web version on PubMed Central for supplementary material.

Acknowledgements

We thank Dr. Mina Bissell, Lawrence Berkley National Laboratory for a gift of casein antibody, Robert Abraham, Wyeth Oncology for interest and support of the project. This work was supported by a collaborative research grant from Wyeth Oncology, shared resource support from the NCI Cancer Center Support Grant 2 P30 CA030199 and R01 CA125255 (MK).

References

Bild AH, Yao G, Chang JT, Wang Q, Potti A, Chasse D, et al. Oncogenic pathway signatures in human cancers as a guide to targeted therapies. Nature. 2006; 439:353–7. [PubMed: 16273092]

Boschelli DH, Ye F, Wang YD, Dutia M, Johnson SL, Wu B, et al. Optimization of 4-phenylamino-3-quinolinecarbonitriles as potent inhibitors of Src kinase activity. J Med Chem. 2001; 44:3965–77. [PubMed: 11689083]

Bracken AP, Helin K. Polycomb group proteins: navigators of lineage pathways led astray in cancer. Nat Rev Cancer. 2009; 9:773–84. [PubMed: 19851313]

Cao Q, Yu J, Dhanasekaran SM, Kim JH, Mani RS, Tomlins SA, et al. Repression of E-cadherin by the polycomb group protein EZH2 in cancer. Oncogene. 2008; 27:7274–84. [PubMed: 18806826]

Cheung ATW, Young LJT, Chen PCY, Chao CY, Ndoye A, Barry PA, et al. Microcirculation and metastasis in a new mouse mammary tumor model system. International Journal of Oncology. 1997; 11:69–77. [PubMed: 21528182]

Coluccia AM, Benati D, Dekhil H, De Filippo A, Lan C, Gambacorti-Passerini C. SKI-606 decreases growth and motility of colorectal cancer cells by preventing pp60(c-Src)-dependent tyrosine phosphorylation of beta-catenin and its nuclear signaling. Cancer Res. 2006; 66:2279–86. [PubMed: 16489032]

Courtneidge SA, Smith AE. Polyoma virus transforming protein associates with the product of the c-src cellular gene. Nature. 1983; 303:435–9. [PubMed: 6304524]

Criscuoli ML, Nguyen M, Eliceiri BP. Tumor metastasis but not tumor growth is dependent on Src-mediated vascular permeability. Blood. 2005; 105:1508–14. [PubMed: 15486073]

Eliceiri BP, Paul R, Schwartzberg PL, Hood JD, Leng J, Cheresh DA. Selective requirement for Src kinases during VEGF-induced angiogenesis and vascular permeability. Mol Cell. 1999; 4:915–24. [PubMed: 10635317]

Ezhkova E, Pasolli HA, Parker JS, Stokes N, Su IH, Hannon G, et al. Ezh2 orchestrates gene expression for the stepwise differentiation of tissue-specific stem cells. Cell. 2009; 136:1122–35. [PubMed: 19303854]

Finn RS. Targeting Src in breast cancer. Ann Oncol. 2008; 19:1379–86. [PubMed: 18487549]

Galang CK, Muller WJ, Foos G, Oshima RG, Hauser CA. Changes in the expression of many Ets family transcription factors and of potential target genes in normal mammary tissue and tumors. J Biol Chem. 2004; 279:11281–92. [PubMed: 14662758]

Golas JM, Lucas J, Etienne C, Golas J, Discafani C, Sridharan L, et al. SKI-606, a Src/Abl inhibitor with in vivo activity in colon tumor xenograft models. Cancer Res. 2005; 65:5358–64. [PubMed: 15958584]

Guy CT, Cardiff RD, Muller WJ. Induction of mammary tumors by expression of polyomavirus middle T oncogene: a transgenic mouse model for metastatic disease. Molecular and Cellular Biology. 1992; 12:954–961. [PubMed: 1312220]

Guy CT, Muthuswamy SK, Cardiff RD, Soriano P, Muller WJ. Activation of the c-Src tyrosine kinase is required for the induction of mammary tumors in transgenic mice. Genes and Development. 1994; 8:23–32. [PubMed: 7507074]

Ishizawar R, Parsons SJ. c-Src and cooperating partners in human cancer. Cancer Cell. 2004; 6:209–14. [PubMed: 15380511]

Ishizawar RC, Miyake T, Parsons SJ. c-Src modulates ErbB2 and ErbB3 heterocomplex formation and function. Oncogene. 2007; 26:3503–10. [PubMed: 17173075]

Jain RK. Normalization of tumor vasculature: an emerging concept in antiangiogenic therapy. Science. 2005; 307:58–62. [PubMed: 15637262]

Jallal H, Valentino ML, Chen G, Boschelli F, Ali S, Rabbani SA. A Src/Abl kinase inhibitor, SKI-606, blocks breast cancer invasion, growth, and metastasis in vitro and in vivo. Cancer Res. 2007; 67:1580–8. [PubMed: 17308097]

Kim H, Chan R, Dankort DL, Zuo D, Najoukas M, Park M, et al. The c-Src tyrosine kinase associates with the catalytic domain of ErbB-2: implications for ErbB-2 mediated signaling and transformation. Oncogene. 2005a; 24:7599–607. [PubMed: 16170374]

Kim H, Laing M, Muller W. c-Src-null mice exhibit defects in normal mammary gland development and ERalpha signaling. Oncogene. 2005b; 24:5629–36. [PubMed: 16007215]

Kim LC, Song L, Haura EB. Src kinases as therapeutic targets for cancer. Nat Rev Clin Oncol. 2009; 6:587–95. [PubMed: 19787002]

Kleer CG, Cao Q, Varambally S, Shen R, Ota I, Tomlins SA, et al. EZH2 is a marker of aggressive breast cancer and promotes neoplastic transformation of breast epithelial cells. Proc Natl Acad Sci U S A. 2003; 100:11606–11. [PubMed: 14500907]

Klein A, Guhl E, Zollinger R, Tzeng YJ, Wessel R, Hummel M, et al. Gene expression profiling: cell cycle deregulation and aneuploidy do not cause breast cancer formation in WAP-SVT/t transgenic animals. J Mol Med. 2005; 83:362–76. [PubMed: 15662539]

Kmiecik TE, Shalloway D. Activation and suppression of pp60c-src transforming ability by mutation of its primary sites of tyrosine phosphorylation. Cell. 1987; 49:65–73. [PubMed: 3103925]

Kouros-Mehr H, Bechis SK, Slorach EM, Littlepage LE, Egeblad M, Ewald AJ, et al. GATA-3 links tumor differentiation and dissemination in a luminal breast cancer model. Cancer Cell. 2008; 13:141–52. [PubMed: 18242514]

Lee TI, Jenner RG, Boyer LA, Guenther MG, Levine SS, Kumar RM, et al. Control of developmental regulators by Polycomb in human embryonic stem cells. Cell. 2006; 125:301–13. [PubMed: 16630818]

Li X, Gonzalez ME, Toy K, Filzen T, Merajver SD, Kleer CG. Targeted overexpression of EZH2 in the mammary gland disrupts ductal morphogenesis and causes epithelial hyperplasia. Am J Pathol. 2009; 175:1246–54. [PubMed: 19661437]

Li Z, Tognon CE, Godinho FJ, Yasaitis L, Hock H, Herschkowitz JI, et al. ETV6-NTRK3 fusion oncogene initiates breast cancer from committed mammary progenitors via activation of AP1 complex. Cancer Cell. 2007; 12:542–58. [PubMed: 18068631]

Lin EY, Jones JG, Li P, Zhu L, Whitney KD, Muller WJ, et al. Progression to malignancy in the polyoma middle T oncoprotein mouse breast cancer model provides a reliable model for human diseases. Am J Pathol. 2003; 163:2113–26. [PubMed: 14578209]

Liu M, Howes A, Lesperance J, Stallcup WB, Hauser CA, Kadoya K, et al. Anti-tumor activity of rapamycin in a transgenic mouse model of ErbB2-dependent human breast cancer. Cancer Res. 2005; 65:5324–5336.

Maglione JE, Moghanaki D, Young LJ, Manner CK, Ellies LG, Joseph SO, et al. Transgenic Polyoma middle-T mice model premalignant mammary disease. Cancer Res. 2001; 61:8298–305. [PubMed: 11719463]

Man AK, Young LJT, Tynan J, Lesperance J, Egeblad M, Hauser CA, et al. Ets2-dependent stromal regulation of mouse mammary tumors. Mol. Cell Biol. 2003; 23:8614–8625. [PubMed: 14612405]

Miyoshi K, Rosner A, Nozawa M, Byrd C, Morgan F, Landesman-Bollag E, et al. Activation of different Wnt/beta-catenin signaling components in mammary epithelium induces transdifferentiation and the formation of pilar tumors. Oncogene. 2002; 21:5548–56. [PubMed: 12165853]

Mukhopadhyay D, Tsiokas L, Zhou XM, Foster D, Brugge JS, Sukhatme VP. Hypoxic induction of human vascular endothelial growth factor expression through c-Src activation. Nature. 1995; 375:577–581. [PubMed: 7540725]

Muthuswamy SK, Siegel PM, Dankort DL, Webster MA, Muller WJ. Mammary tumors expressing the *neu* proto-oncogene possess elevated c-Src tyrosine kinase activity. Molecular and Cellular Biology. 1994; 14:735–743. [PubMed: 7903421]

Neznanov N, Man AK, Yamamoto H, Hauser CA, Cardiff RD, Oshima RG. A single targeted Ets2 allele restricts development of mammary tumors in transgenic mice. Cancer Res. 1999; 59:4242–6. [PubMed: 10485465]

Oshima RG, Lesperance J, Munoz V, Hebbard L, Ranscht B, Sharan N, et al. Angiogenic Acceleration of Neu Induced Mammary Tumor Progression and Metastasis. Cancer Res. 2004; 64:169–179. [PubMed: 14729621]

Remsing Rix LL, Rix U, Colinge J, Hantschel O, Bennett KL, Stranzl T, et al. Global target profile of the kinase inhibitor bosutinib in primary chronic myeloid leukemia cells. Leukemia. 2009; 23:477–85. [PubMed: 19039322]

Rosner A, Miyoshi K, Landesman-Bollag E, Xu X, Seldin DC, Moser AR, et al. Pathway pathology: histological differences between ErbB/Ras and Wnt pathway transgenic mammary tumors. Am J Pathol. 2002; 161:1087–97. [PubMed: 12213737]

Rudolph MC, McManaman JL, Phang T, Russell T, Kominsky DJ, Serkova NJ, et al. Metabolic regulation in the lactating mammary gland: a lipid synthesizing machine. Physiol Genomics. 2007; 28:323–36. [PubMed: 17105756]

Schwartzberg PL, Xing L, Hoffmann O, Lowell CA, Garrett L, Boyce BF, et al. Rescue of osteoclast function by transgenic expression of kinase-deficient Src in src−/− mutant mice. Genes Dev. 1997; 11:2835–44. [PubMed: 9353253]

Silva CM, Shupnik MA. Integration of steroid and growth factor pathways in breast cancer: focus on signal transducers and activators of transcription and their potential role in resistance. Mol Endocrinol. 2007; 21:1499–512. [PubMed: 17456797]

Spector DH, Varmus HE, Bishop JM. Nucleotide sequences related to the transforming gene of avian sarcoma virus are present in DNA of uninfected vertebrates. Proc Natl Acad Sci U S A. 1978; 75:4102–6. [PubMed: 212733]

Summy JM, Gallick GE. Treatment for advanced tumors: SRC reclaims center stage. Clin Cancer Res. 2006; 12:1398–401. [PubMed: 16533761]

Varambally S, Cao Q, Mani RS, Shankar S, Wang X, Ateeq B, et al. Genomic loss of microRNA-101 leads to overexpression of histone methyltransferase EZH2 in cancer. Science. 2008; 322:1695–9. [PubMed: 19008416]

Vultur A, Buettner R, Kowolik C, Liang W, Smith D, Boschelli F, et al. SKI-606 (bosutinib), a novel Src kinase inhibitor, suppresses migration and invasion of human breast cancer cells. Mol Cancer Ther. 2008; 7:1185–94. [PubMed: 18483306]

Watkin H, Richert MM, Lewis A, Terrell K, McManaman JP, Anderson SM. Lactation failure in Src knockout mice is due to impaired secretory activation. BMC Dev Biol. 2008; 8:6. [PubMed: 18215306]

Webster MA, Cardiff RD, Muller WJ. Induction of mammary epithelial hyperplasias and mammary tumors in transgenic mice expressing a murine mammary tumor virus/activated c-src fusion gene. Proc Natl Acad Sci U S A. 1995; 92:7849–53. [PubMed: 7544006]

Webster MA, Hutchinson JN, Rauh MJ, Muthuswamy SK, Anton M, Tortorice CG, et al. Requirement for both Shc and phosphatidylinositol 3′ kinase signaling pathways in polyomavirus middle T-mediated mammary tumorigenesis. Mol Cell Biol. 1998; 18:2344–59. [PubMed: 9528804]

Weis S, Cui J, Barnes L, Cheresh D. Endothelial barrier disruption by VEGF-mediated Src activity potentiates tumor cell extravasation and metastasis. J Cell Biol. 2004; 167:223–9. [PubMed: 15504909]

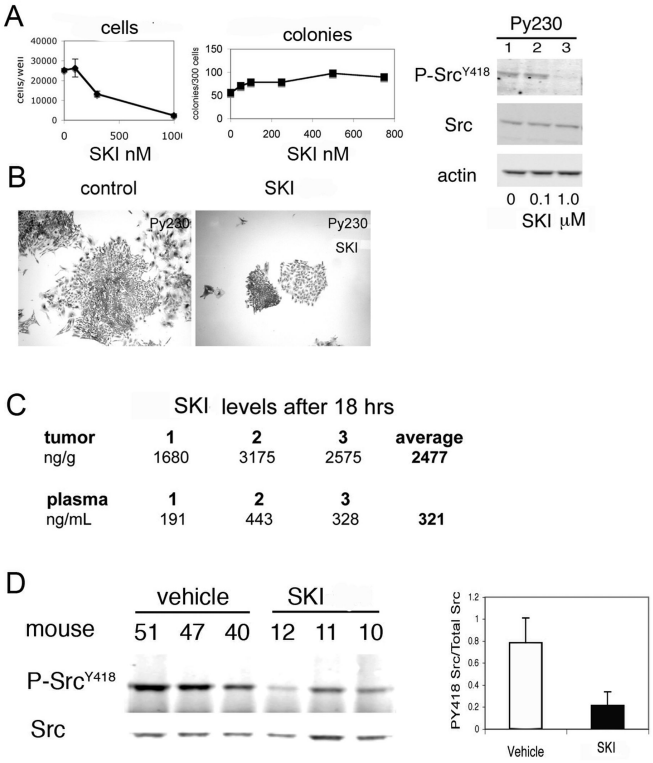

Figure 1.

SKI-606 effects on Py-230 cells and Src phosphorylation. A, concentration dependence of SKI-606 on cell growth and cloning efficiency of the Py-230 mammary tumor cell line. Immunoprecipitation and western blot analysis show the effect of SKI-606 on phosphorylated Src in Py-230 cells. B, morphology of Py-230 clones in control or 500 nM SKI-606. C, SKI-606 levels in tumors and plasma 18 hours after treatment of tumor-bearing MMTV-PyMT females. D, phosphorylation state of Src in tumors from vehicle and SKI-606-treated animals. Representative western blot images of Src signals of tumors from animals receiving the vehicle or SKI-606. Bar graph shows the mean and standard deviation of signals of Src phosphorylated on tyrosine 418 (PY418 Src) normalized to total Src.

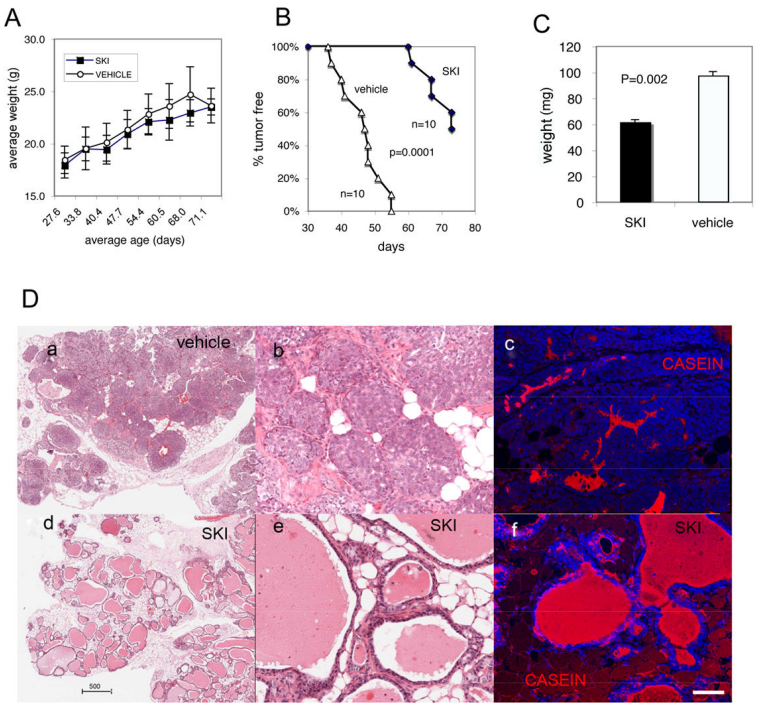

Figure 2.

Suppression of tumor appearance by SKI-606. A, average weight of animals treated with SKI-606 or vehicle. Error bars indicate standard deviations of binned ages as indicated. B, tumor incidence. The P value was calculated by the log rank test. C, weight of tumor-free mammary gland. The fourth inguinal mammary glands that had no discrete tumor mass were excised and weighed. D, sections of mammary tumors (a, b, c) from control mice and of the mammary glands of SKI-606-treated mice (d, e, f) were either stained with HE (a, b, d, e) or with antibody to beta-casein (red) (c, f) and DAPI (blue).

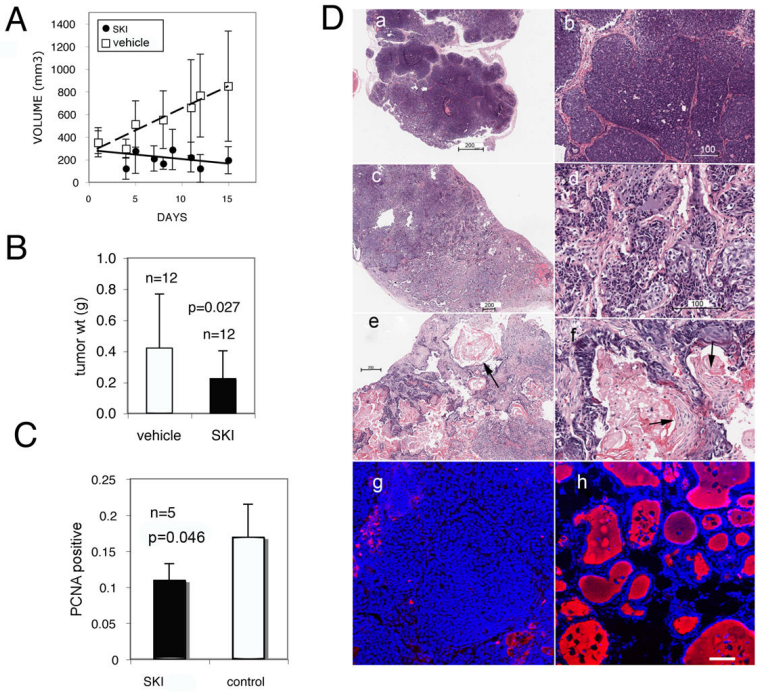

Figure 3.

Effect of SKI-606 on fully developed tumors. A, Tumor size was measured at the indicated time of treatment starting with tumors of approximately 1 cm in diameter. The average and standard deviations are shown for groups binned for elapsed time of treatment for clarity. Linear regression analysis of all data indicated an extremely significant difference in the slopes of the two lines. Both slopes were also judged differ from zero. B, average weight of excised tumors after 14 days of treatment. C, proliferative cell nuclear antigen (PCNA) was detected by antibody staining of tumor sections. Average and standard deviation of the nuclei fraction stained positive for PCNA. D, increased diversity of tumor histology after treatment with SKI-606 for 14 days. Control tumors are shown in D-a, D-b and D-g. Tumors from SKI-606-treated mice are shown in panels D-c, D-d, D-e, D-f and D-h. Panels D-a through D-f show sections stained with hematoxylin and eosin. Panels D-g and D-h show staining for beta-casein (red) and nuclei (blue). Arrows in panels D-e and D-f, point to keratinizing epithelium.

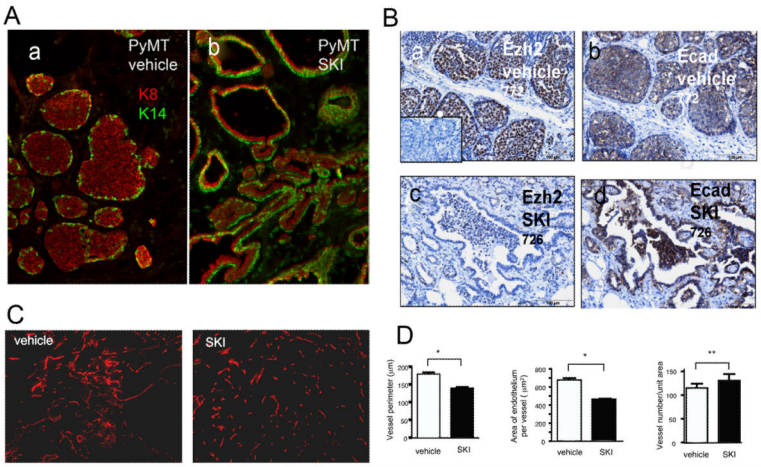

Figure 4.

Keratin, Ezh2 and CD31 expression in tumors treated with SKI-606 for 14 days. Luminal epithelial lineages (K8, red) and basal-like epithelia (K14, green) were visualized in sections of tumors of mice treated with vehicle (A-a) or SKI606. (A-b). B, localization of Ezh2 and E-cadherin in tumors. Lower panels show decreased Ezh2 expression of SKI-606-treated tumors. C, CD31 (red) staining of tumor sections. SKI-606-treated tumor (right) has more organized and regular spacing. D, image analysis reveals length of vessel perimeter (left), endothelium area of vessel (middle), by t-test and vessel density (right). *P < 0.001, ** P = 0.32 calculated by T-test. Average values and standard errors are indicated.

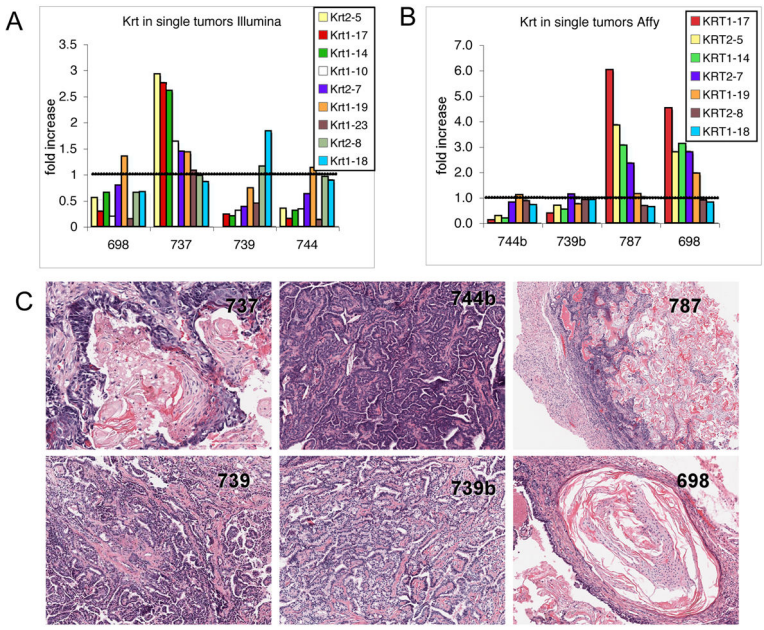

Figure 5.

Variability of differentiation induced by SKI-606. Bisected tumors were fixed, sectioned and stained with HE. RNA was isolated from half of the tumor and analyzed by either Illumina or Affymetrix array methods. A, normalized individual RNA sample results for keratin RNAs. The fold increase in expression is relative to the average of four control PyMT tumor RNA samples. Tumors are identified by the indicated animal number with appended letters for multiple tumors isolated from individual animals. B, keratin RNAs detected by Affymetrix array methods of the indicated tumors. C, histological detection of epidermal keratin differentiation. Epidermal differentiation was noted in tumors 737, 787 and 698 which corresponds to increased keratin 5, 14 and 17 RNA detected by both arrays.

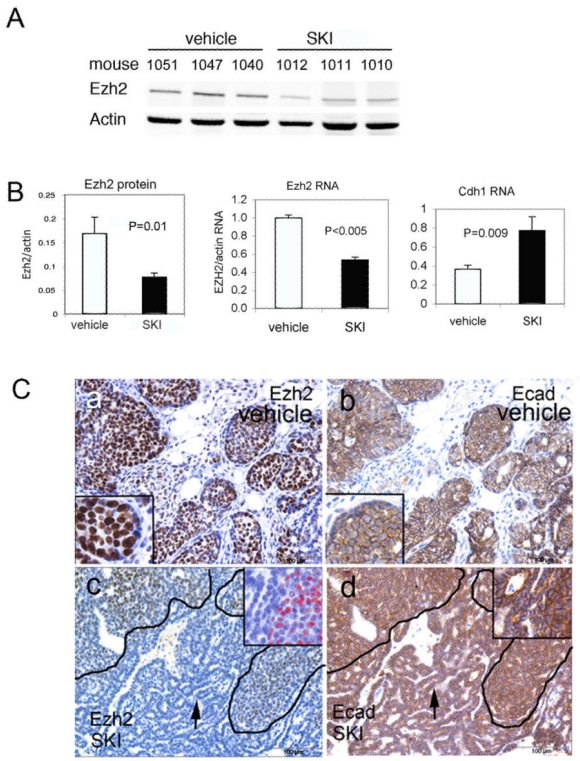

Figure 6.

Suppression of Ezh2 by SKI-606 treatment. MMTV-PyMT tumor-bearing animals were treated once with SKI-606 and analyzed 18 hour later. A, filter image of Ezh2 and actin signals. B, mean and standard deviation of Ezh2 protein signals normalized to actin. Values represent the average and standard deviation of six values from three treated and control tumors. Ezh2 and Cdh1 RNAs were measured by Q-rtPCR normalized to actin or cyclophilin RNA levels. Bars represent the mean and standard deviation of relative RNA from three or four tumors each. P value represents the results of T-test. C, immunohistochemical localization of Ezh2 and E-cadherin in sections of tumors treated with vehicle or SKI-606. Brown color reveals reaction with the indicated antibodies. In C-c and C-d solid tumor areas reactive with the Ezh2 antibody are indicated with drawn lines. Areas not reactive with Ezh2 appear in greater epithelial organization (arrows). The digitally magnified inset in panel C-c has the brown color replaced with red for clarity of boundary between a reactive and non-reactive portion of the tumor. Insets in panels C-a, C-b and C-d are digitally magnified to reveal the nuclear localization of Ezh2 and the junctional location of E-cadherin antibody reaction.